

Humidification Degree Effect under Rain of Inclined Silicone Insulation on its Electric Performance

Samia Slimani^{1*}, Abdellah Medjdoub¹, Stefan Kornhuber²

¹ Laboratory of Electrical Engineering, Faculty of Technology, University of Bejaia, 06000 Bejaia, Algeria

² Faculty of Electrical Engineering and Informatics, University of Applied Sciences Zittau/Görlitz, Theodor-Koerner-Allee 16, 02763 Zittau, Germany

* Corresponding author, e-mail: samia.slimani@univ-bejaia.dz

Received: 13 October 2022, Accepted: 20 September 2023, Published online: 28 November 2023

Abstract

This investigation is focused on the effect of inclination angle with respect to the horizontal of a hydrophobic silicone insulation, on the rate of its creepage distance's wetting by natural rain. The constellation of rainwater drops obtained on the de-energized site is then reproduced in the laboratory, to quantify the effect of their volume on the humidification intensity of the inclined insulation's creepage distance, and therefore its electrical performance under different alternating voltage levels. For this purpose, two different experimental devices allowing the variation of the insulation's inclination angle were set-up. The first one is dedicated to the on-site display of silicone samples in natural rain. The second one allows the study of the applied voltage's effect on the wetting degree of the insulation's surface. All the performed tests were supported by camera visualization. On-site measurement results show a decline in the length of the creepage distance of the natural rain-wetted insulation with increasing its inclination angle. Laboratory results also show a decrease in the size of the insulation's wet surface with increasing its inclination angle. These two characteristics reveal two different intervals of critical inclination angles of the insulation, unfavorable and favorable, for the dimensioning of the insulators' sheds corresponding respectively to their minimum and maximum electrical performance.

Keywords

flashover, discharge, AC voltage, silicone insulation, rainwater drops, inclination angle

1 Introduction

The continuity of service and the quality of electrical power is ensured by the reliability of the transmission line protection insulators.

The optimal exploitation of electrical insulators depends on their correct sizing and choice according to basic criteria, taking into consideration environmental constraints, in particular pollution [1, 2]. Indeed, the atmospheric emissions covering an insulator can become humid when in contact with dew droplets, rain or fog. This can result in an intense current leakage to the ground, which in turn can cause damage to the equipment connected to the electrical network [1, 2].

The easy and quick wetting of ceramic insulators leads to a negative impact on their insulating capacity [2, 3]. This is due to the formation of continuous water films on their hydrophilic surface, which drastically reduces their dry insulation path and increases the risk of electric discharge propagation. In order to reduce the degree of

wettability of their surface, silicone insulators have been widely used during the last six decades in these electric power transmission lines [4, 5].

Due to the hydrophobicity quality of their surface, discrete water droplets form on them in rain or fog. As a result, the distribution of the conductive pollutant deposit dissolved in the liquid becomes discontinuous and dry areas are created on their surface along their creepage distance.

The resulting leakage currents could be severely limited and electric discharges are reduced even under extreme pollution conditions. In addition, the light weight, very high resistance to contamination and mechanical stress are characteristics proving the excellence of such materials for high and medium electrical voltage applications [6–8].

On the other hand, the disadvantage most cited by researchers is the loss of hydrophobicity of this type of material causing its long-term deterioration following the recurrence and persistence of climatic phenomena under

operating voltage. This is probably due to the development of partial electric discharges, which are generated following the deformation of the water drops by the applied electric field under operating voltage [9–11].

Under natural rain, there is very little published work on the AC and DC electrical performance of silicone insulators as a function of the inclination angle of their sheds [12–14]. Under artificial rain, the existing tests are those carried out in AC voltage on real silicone insulators, at the standard inclination angle of their sheds [15, 16].

In these tests, the humidification process of insulators is described as a phenomenon of water drops colliding with the surface of an insulator and their diffusion on this one. The rate of humidification of its creepage distance is probably related to the number of rainwater drops, their size, their angle of fall, the distance between them, and their impact speed on the surface and the inclination of the fall point from the horizontal.

From this review, we can conclude that the effect of any inclination of such insulators' sheds, on the degree of humidification of their creepage distance has not been sufficiently investigated and still requires further research. This constitutes one of the obvious reasons, which lead us to quantify this parameter in this study. The experimental investigation concerns the influence of the inclination angle of the surface of hydrophobic silicone insulation on the wetting's rate of its creepage distance under natural rain. The constellation obtained from natural rainwater drops is then reproduced in the laboratory to quantify the effect of their volume on the humidification intensity of the inclined insulation creepage distance and therefore its electrical performance out or under a variable alternating voltage level.

On the technical and economic plan, using of high-performance electrical insulators in electrical installations impacts companies by reducing their energy consumption and associated costs, since energy losses due to leakage current can make up a significant part of the electricity bill and save companies money. By eliminating energy losses, equipment operates more efficiently and consumes less energy. It can also extend the life of equipment, reducing maintenance and replacement costs. On the other hand, the risk of fire and electrocution is reduced, which can improve workplace safety and thus worker safety.

2 Experimental devices and measurement techniques

In order to establish a relationship between the degree of wetting of the insulator's creepage distance and the inclination angle of its sheds compared to the horizontal, measurements of the impact volume of natural rainwater drops on

their surface were carried out. As the material of the insulation, the choice is made on silicone. Its geometry resembles a half-shed and the length of its creepage distance is equal to 6 cm, Fig. 1. Samples of this insulation were cut from a new silicone insulator with 3 alternating sheds.

In order to allow the comparison of the humidity rate of the top and the bottom of two distinct creepage distances of the same insulation, four sectors of 1 cm² in area foreach were chosen and their location on the insulation's surface is illustrated by Fig. 1. The choice of their location was made so that a sector is placed at each end of the creepage distance of the insulation going from the middle to the periphery of the half-shed. For a given duration of exposure time of the samples to natural rain, measurements were made to characterize the water drops formed on each of the four sectors according to their size (large, medium and small) and their number. In order to ensure the reproducibility of the quantified quantities, these measurements were carried out during three distinct periods of natural rain.

During each of these three selected time periods, a quantity of rainwater was collected in a bucket and its electrical conductivity was measured using a mobile probe conductivity meter. Its value is 30 μ S/cm. It is practically identical for the three periods.

The volume of all the water drops recorded on each of the four sectors of the insulation is measured using a 5 μ l glass syringe. The spare needle of the latter is made of stainless steel, brand SGE and its weight is 0.00085 Kg (Fig. 2). The interval break in proceeding between testing a sample and its new exposure to natural rain is greater than 12 h. This was chosen to allow the sample used to completely recover the hydrophobicity of its surface before its new exposure [17]. To accelerate this return of hydrophobia, all the samples are placed, after cleaning with isopropanol, in a desiccator at the end of each series of measurements.

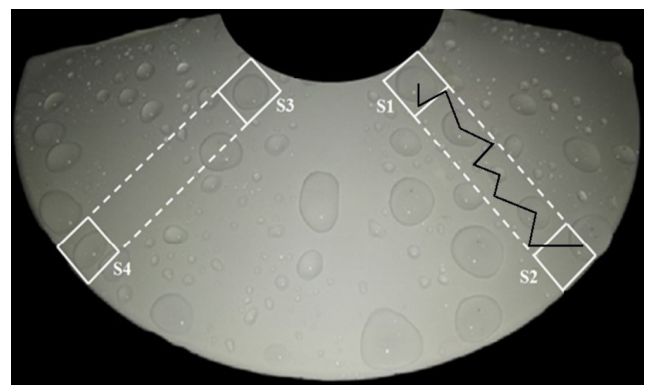


Fig. 1 Location of four sectors (S_1 , S_2) and (S_3 , S_4) on two creepage distances of a silicone half-shed covered with natural rainwater drops



Fig. 2 Measurement of the natural rainwater drops' volume using a glass syringe (SGE) graduated in microliter

The variation of the insulation's inclination angle compared to the horizontal (α) is obtained on site by means of a device illustrated in Fig. 3.

The rods are numbered from left to right and the displayed tilt angles are shown in Fig. 3. The impact phenomenon of natural raindrops on the insulation's surface and their resulting constellation, were filmed during each rain period using a camera.

In order to reproduce in the laboratory, the constellation of natural raindrops and their resulting volume, tests were carried out on silicone insulations of the same nature as those used on site. They are parallelepiped with dimensions $(11 \times 11 \times 0.6)$ cm³ and delimited by a geometry of flat electrodes with a quasi-uniform electric field (Fig. 4 (a) and Fig. 4 (b)). These silicone surfaces are products based

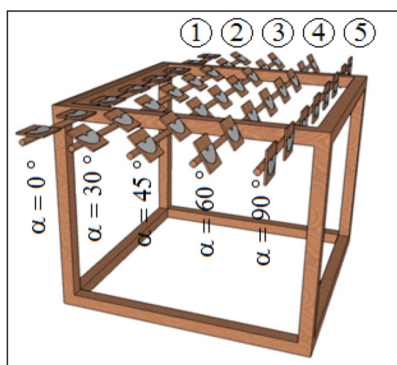


Fig. 3 Device with five rotating cylindrical rods ensuring the variation of the inclination angle compared to the horizontal of the silicone insulation

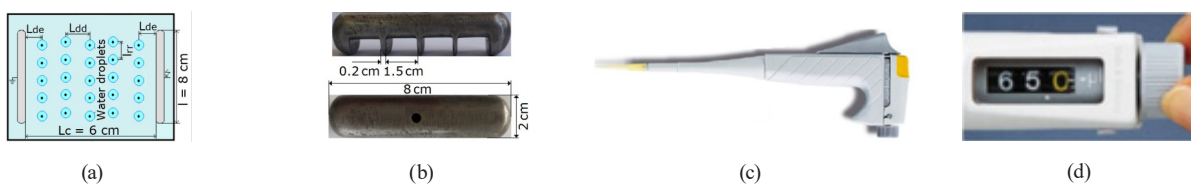


Fig. 4 Zigzag arrangement of water drops on a silicone sample delimited by two electrodes and a micropipette (a) Experimental setup, (b) Toothed HV and ground electrodes, (c) Graduated pipette, (d) Volume adjustment from 10 to 100 μ l

on high temperature vulcanization rubber, mixed with aluminum trihydrate at a rate of 4 to 5%. The static contact angle of a 5 μ l water drop laying on its surface is estimated at 104° according to the German company Wacker Chemie, supplier and manufacturer of these samples [18, 19]. During this study, the number of test samples is taken equal to 20.

The electrodes are made of iron, one is connected to the ground and the other one to high voltage. The width (l) of the electrodes is 8 cm, their diameter (ϕ_e) is 2 cm and their radius of curvature (r_c) is equal to 1 cm. The base of the electrodes is cut into teeth with a thickness of 0.2 cm. They are spaced of 1.5 cm apart to facilitate the evacuation to the outside of water drops coming into contact with them (Fig. 4 (b)). The total insulation creepage distance (L_c) between the electrodes is set at 6 cm throughout the tests carried out (Fig. 4 (a)).

The impact point of each water drop on the surface of the insulation was previously identified using an insulating black tint. The symmetrical zigzag arrangement of water drops on the interelectrode surface of the insulation is described by parameters (L_{dd}), (L_{de}) and (l_{rr}) (Fig. 4 (a)). They are kept constant throughout the tests carried out in this study. Their values are respectively: $L_{dd} = 1$ cm, $L_{de} = 1$ cm and $l_{rr} = 2$ cm.

The results of the variation's effect of these parameters on the electrical performance in AC and DC voltage of the same insulation in horizontal position have already been published under the reference [14].

The deposition of the water drops on the insulating surface was carried out using a micropipette. The water drops' volume initially deposited (V_{di}) chosen, is taken almost equal to that found during measurements carried out under natural rain (45, 60, 90 and 120) μ l (Fig. 4 (c)). The electrical conductivity of the water drops is set equal to 30 μ S/cm [20].

The device realized in the laboratory, allowing the variation of the inclination angle (α) of the insulation compared to the horizontal is illustrated in Fig. 5. It is made of wood with $(50 \times 50 \times 40)$ cm³ in dimensions. The insulation is immobilized on the top base wall of the device. This is connected to a ball joint allowing it to describe an angle (α), between 0 and 90°.

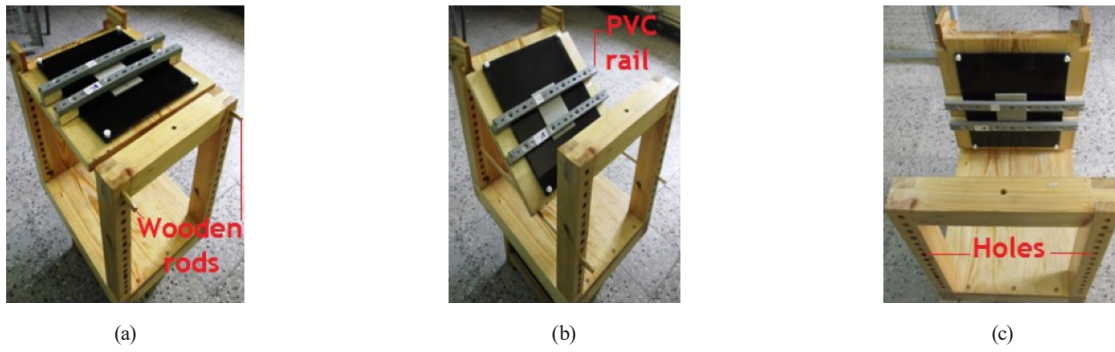


Fig. 5 Device with rotating upper wall ensuring the variation of the inclination angle (α) of the insulation compared to the horizontal (a) $\alpha = 0^\circ$, (b) $0^\circ < \alpha < 90^\circ$, (c) $\alpha = 90^\circ$

The experimental model and the electrical circuits for measuring the different voltage levels applied to the insulation and for visualizing the electric discharge evolving on its surface are illustrated in Fig. 6.

In order to determine the moisture content of the insulation's creepage distance, voltage is applied to the sample in stages. The value of the voltage level is obtained by automatic variation of the voltage ramp at a constant speed equal to 4 kV/s. Two voltage levels (10 and 28 kV), lower than that of its flashover, were chosen.

In the case of determining the electrical performance of the insulation, the test voltage is automatically increased at constant ramp speed until the flashover of its total surface. After each test, the volume of the various residual water drops still adhering to the material's surface is measured using a syringe graduated in microliters.

For each influence parameter investigated in this paper, a series of 20 tests were carried out and the retained value of the flashover voltage of the insulation is the arithmetic average of all those obtained on the same series of measurement. The calculation of the mean value and the standard deviation of the silicone insulation's flashover voltage as a function of each influencing parameter was carried out on the basis of Eq. (1) and Eq. (2) [21]:

$$U_{fm} = \frac{\sum_1^N U_{ifm}}{n} \quad (1)$$

$$RSD = \sqrt{\frac{\sum_1^N (U_{ifm} - U_{fm})^2}{N-1}} \cdot \frac{100\%}{U_{fm}}, \quad (2)$$

where U_{fm} is the average of the measured flashover voltage of the insulation (kV); U_{ifm} is the applied voltage obtained from the test in the time of i (kV); N is the total times of the valid test, $N = 20$; RSD is the relative standard deviation of the test result.

All results obtained in this study were brought back to the following normal conditions ($\theta_0 = 20^\circ\text{C}$, $P_0 = 100\text{ kPa}$ and $H_0 = 11\text{ g/m}^3$) in accordance with the equations and charts existing in the literature [22].

$$U_{fm} = \frac{K_H}{K_d} U_{fm} \quad (3)$$

U_{fm} is the flashover voltage measured at temperature θ , pressure P and humidity H . U_f is the flashover voltage under normal conditions (θ_0 , P_0 and H_0).

K_H is the correction factor relating to humidity. Its value is deduced from the charts given in [21]. K_d is the correction factor relating to the temperature and the pressure whose expression has the form:

$$K_d = \frac{2.93P}{(273 + \theta)} U_{fm}, \quad (4)$$

where P (pressure) is in kPa and θ (temperature) in $^\circ\text{C}$.

The good repetition of the measurement techniques allowed us to have maximum relative error equal to 5% of the arithmetic average value.

A break lasting more than 12 hours is observed between two successive tests on the same specimen in order to restore the hydrophobicity of the sample's surface after it has been put under voltage [17]. In order to speed up the

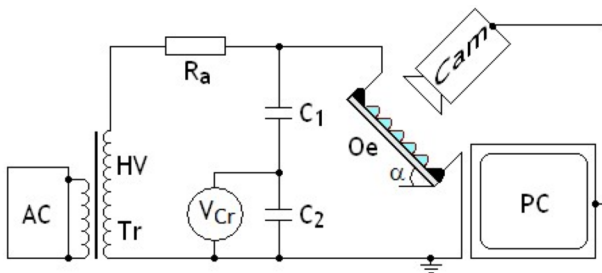


Fig. 6 Diagram of voltage level measurement applied to the insulation and visualization of the electric discharge evolving on its surface (Tr: Transformer; AC: Test voltage control device; Vcr: Peak voltmeter, Oe: test object; Cam: Camcorder; PC: Computer)

process, the twenty samples are always placed in a desiccator after cleaning with isopropanol after each series of tests.

3 Results and discussion

3.1 Humidification degree under natural rain of insulation with a variable inclination angle

The evolution of the volume of water drops collected on sector S_1 (Fig. 1) as a function of their size and the exposure time of the different insulation samples under natural rain is illustrated in Fig. 7. Its resulting characteristic is of sawtooth shape regardless of the water drops' size. Indeed, following the phenomenon of collision of rainwater drops with the insulation's surface, at any inclination angle and their diffusion on it, the quantity of water collected per cm^2 of its surface increases to reach a maximum volume corresponding to the peaks generated.

This maximum volume is defined as the quantity of water that can still adhere to its point of impact on the insulation when de-energized under the effect of gravitational and hydrodynamic forces. The value of these volume peaks of large water drops is also a function of the insulation's inclination, the wind and the temperature. In the absence of voltage, large and heavy water drops end up falling under the effect of the resulting forces, leaving behind water droplet residues. If at this time the rain continues to fall, the residual water volume is again raised more or less to its maximum value by that of the natural rainwater drops falling on the same place. On the other hand, if the rain stops falling, the maximum accumulated water volume will begin to decrease because of its evaporation until the total drying out of the impact surface at high temperature and/or its ejection completely from the point of impact by wind. However, during its decrease, it can also reach a lower value shown in Fig. 7. This is defined as being the quantity

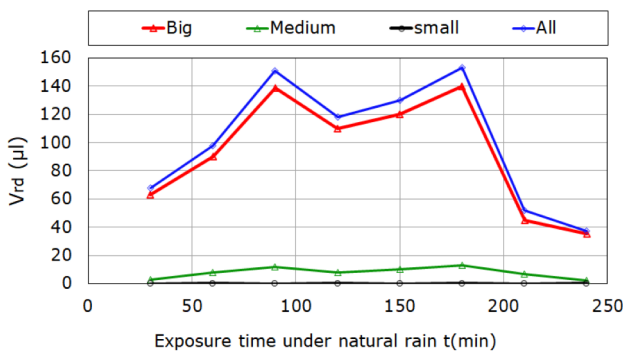


Fig. 7 Residual volume of water drops collected in sector S_1 depending on their size and the time of exposure of the insulation to natural rain ($\alpha = 0^\circ$, P_1 : 10/02/2018)

of water recorded between the stopping time of the first rain and the resumption of the rain next. So, if the rain resumes its fall without interruption during the decrease in this water volume, it increases again until it reaches its maximum value. This clearly explains the sawtooth geometry of the characteristic illustrated in Fig. 7.

As for the medium and small drops, they are generally created during the bursts of natural rainwater drops following their successive impacts on the surface's insulation.

Fig. 7 also shows that the volume of large water drops is equal to 93% of the total volume harvested in area S_1 . On the other hand, that of medium and small water drops is respectively only 6.6% and 0.4% of the total volume. The largest drops in a sector are always targeted along the creepage line (Fig. 1). In the absence of voltage, the maximum volume of large water drops, which can be formed on the surface of an insulation in horizontal position ($\alpha = 0^\circ$), is of the order of 140 μl . This is reached after 90 minutes of uninterrupted natural rainfall and this peak is reproduced in a similar way during the second rain (Fig. 8). So, the large drops of natural rainwater play a very decisive role in the degree of humidity of the insulation's creepage distance and therefore its electrical performance.

Fig. 8 gives the evolution of natural rainwater drops' volume collected on area S_1 , on 10/02/2018 for inclination angles of the insulation corresponding respectively to $\alpha = 45^\circ$ and 90° . This results in sawtooth shapes, similar to those obtained for the same insulation in a horizontal position ($\alpha = 0^\circ$) (Fig. 9). The two curves show two volume peaks of natural rainwater drops, depending on the inclination angle of the insulation's surface. This is reached after 90 minutes, during each of the two successive rains regardless of the inclination angle of the insulation. For $\alpha = 45^\circ$, the maximum value of residual water drops' volume that can still adhere to the surface of the

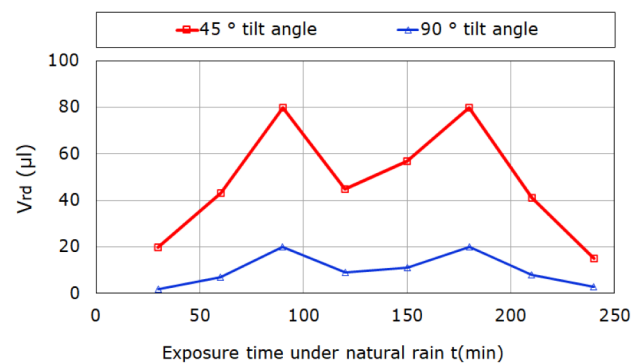


Fig. 8 $V_{rd} = f(t)$ for the S_1 sector of the silicone insulation ($\alpha = (45^\circ, 90^\circ)$, P_1 : 10/02/2018)

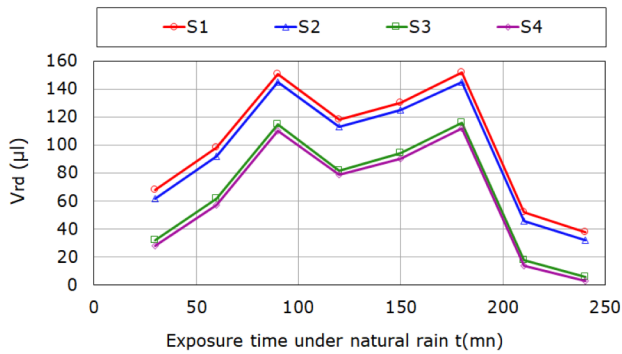


Fig. 9 $V_{rd} = f(t)$ for the four areas S_1, S_2, S_3 and S_4 of the silicone insulation ($\alpha = 0^\circ, P_1: 10/02/2018$)

insulation is $80 \mu\text{l}$. This volume is decreasing, and its maximum value is of the order of $20 \mu\text{l}$ for $\alpha = 90^\circ$. The shape of these curves is similar to those obtained in the case of silicone insulation inclined at an angle of 20° and exposed to natural rain [12, 22].

The Fig. 10 illustrates the flashover arc width on the insulations covered with water drops at varying inclination.

The results of the comparison of residual water drops' volumes from natural rain, collected on sector S_1 of the insulation during the three measurement periods, are summarized in Fig. 11. This results in the curves' appearance in the form of sawtooth whatever the time period considered. The two curves relating to the periods: 10/02/2018 and 21/01/2019, each of them has two maximum values separated by a lower value and the curve relating to the period: 11/01/2019 has only

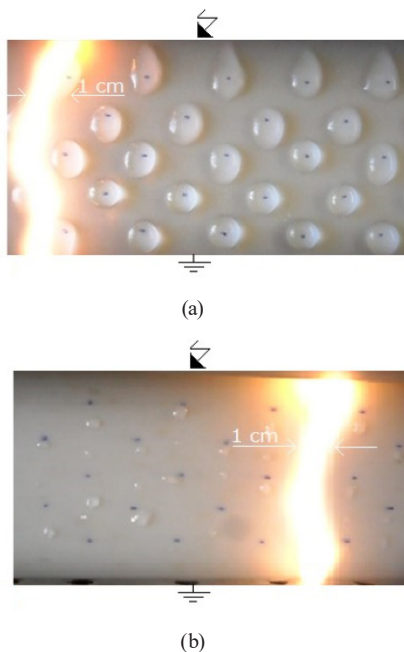


Fig. 10 Channel width of the flashover arc of the silicone insulation's surface covered with water drops at varying inclination angles (a) $\alpha = 0^\circ$, (b) $\alpha = 45^\circ$

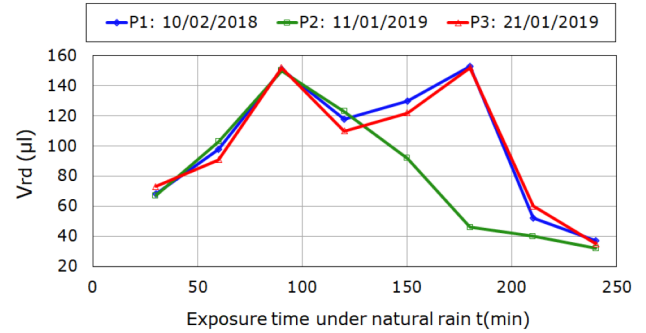


Fig. 11 $V_{rd} = f(t, P)$ of the residual water drops from natural rain collected on the S_1 area of the silicone insulation ($\alpha = 0^\circ$)

one. As it was said previously, the existence of two peaks on the same curve separated by a minimum is explained by the fall of two successive rains and the presence of a single peak corresponds to the fall of a single rain.

In Fig. 11, the reproduction of the maximum value of $152 \mu\text{l}$ of the peak is observed from one rain to another during the same period and from one measurement period to another. The stability of these values is justified by that of the values of temperature, relative humidity and wind speed represented in Table 1, blowing from the creepage distance (S_3, S_4) towards (S_1, S_2).

Fig. 12 gives the evolution of the residual drops' volume of natural rainwater collected on the sector S_1 of the silicone insulation (V_{rd}) as a function of the inclination angle of its surface compared to the horizontal (α) and the time period (P) of its exposure. This results in a slight decline of

Table 1 Climatic conditions during periods of natural rain

Period	10/02/2018	11/01/2019	21/01/2019
Temperature (C°)	8 to 9	7 to 8	10
Wind (km/h)	27	25	26
Relative humidity (%)	85 to 90	86 to 92	87 to 92
Total rain volume (ml)	420	350	380

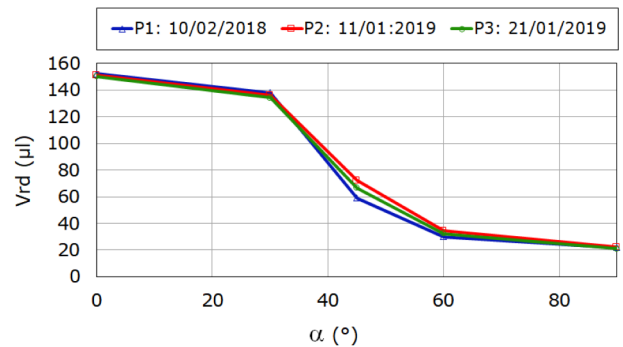


Fig. 12 Volume of residual rainwater drops collected on sector S_1 as a function of the inclination angle of the insulation and the period of its exposure

it to an inclination angle (α) equal to 30° , its strict decrease when $30^\circ < \alpha < 60^\circ$ and another slight decline of this volume when $60^\circ \leq \alpha \leq 90^\circ$, regardless of the time period of exposure considered in this study.

Water drop is in motion on a surface of hydrophobic insulation without voltage and inclined by an angle (α), according to Naiver-Stokes, subjected to the set of forces given by Eq. (5) [23, 24]:

$$\rho \left(\frac{\partial \vec{V}_f}{\partial t} + \vec{V}_f \cdot \nabla \vec{V}_f \right) = -\nabla P_\Delta + \mu \nabla^2 \vec{V}_f + \vec{F}_g, \quad (5)$$

where ρ , V_f and μ respectively characterize the density of the fluid, its velocity and its viscosity. The three terms ∇P_Δ , $\mu \nabla^2 \vec{V}_f$ and \vec{F}_g , respectively represent the effects of forces due respectively to the pressure, viscosity and gravitational force exerted on the water drop.

Equation (5) can also be written in the following form [23]:

$$\rho \left(\frac{\partial \vec{V}_f}{\partial t} + \vec{V}_f \cdot \nabla \vec{V}_f \right) = mg \sin \alpha - F_{ad} - F_s - F_d, \quad (6)$$

where F_{ad} , F_s and F_d are the forces of adhesion, shearing and air drag. These three forces are described respectively by Eqs. (7)–(9):

$$F_{ad} = \frac{25}{\pi^3} \gamma_{LV} D (\cos \theta_R - \cos \theta_A), \quad (7)$$

where D is the diameter of the droplet, γ_{LV} is the surface voltage, θ_R is the droplet retreat angle, θ_A is the droplet advancement angle.

A shearing force is generated when the droplet slides on a surface due to the strain rate of the fluid formed along the contact line between the water droplet and the hydrophobic surface. This can be written in the following form:

$$F_s = A_w \left(\mu \frac{dV}{dy} \right), \quad (8)$$

where A_w is the contact area of the drop, μ is the viscosity of the liquid in the droplet, V is the speed of the flow, and y is the normal distance to the contact area.

The drag force, due to the resistance of the air as the droplet slides over a surface, is related to the drag pressure and friction, due to sliding. It can be of the form:

$$F_d = \frac{1}{2} C_d \rho_a A_c U_T, \quad (9)$$

where C_d is the drag coefficient, ρ_a is the density of air, A_c is the cross-sectional area of the droplet, and U_T is the

translational speed of the droplets along the sloping surface of the insulation.

A residual drop of rainwater remaining motionless on the surface of the insulation, inclined at an angle (α), must meet the conditions of equilibrium according to Eq. (10):

$$mg \sin \alpha - F_{ad} - F_s - F_d = 0. \quad (10)$$

In fact, when a sample is taken, the volume of any residual water droplets (V_d) still adhering to the insulation surface is created following the phenomena of collision and diffusion of rainwater drops [15, 16]. Knowing that the volume varies in the same direction as the mass ($m_d = m_{vd} V_d$), to the coefficient close to the density of the raindrop (m_{vd}), so if (α) increases, the volume (V_d) or the mass (m_d) of the residual water drop must decrease so that the conservation of its equilibrium is guaranteed. This is verified since the intensity of the three forces (F_{ad}), (F_s) and (F_d) decreases with the decrease in the volume (V_d) of the drop due to their connection by the diameter of the latter according to the respective Eqs. (7)–(9). This clearly explains the decrease in the shape of the characteristic $V_{rd} = f(\alpha)$, illustrated in Fig. 12.

The highest volume ($V_d = 140$ to $152 \mu\text{l}$) is recorded practically when the surface of the sample is in a horizontal position ($\alpha = 0^\circ$) or inclined at an angle (α) between 0 and 30° , then the small volume ($V_d = 20$ to $30 \mu\text{l}$) is obtained for $60^\circ \leq \alpha \leq 90^\circ$. The ratio of these two volumes is at most equal to 7.5. This means that the creepage distance of the insulation in horizontal position is 7.5 times wetter than that found in a vertical position. So, the most likely flash-over of the insulation under voltage can occur within this interval of its surface inclination angle. Therefore, when sizing silicone insulators, it is not recommended to use this interval of inclination angle of their sheds, which favors the accumulation of a lot of water on their surface in this case. On the other hand, the most favorable inclination angle for these insulators corresponds to α greater than or equal to 60° (Fig. 12).

The evolution of the residual drops number of natural rainwater recorded on the surface of area S_1 of the insulation (N_{rd}) as a function of its inclination angle (α) and the time period (P) of its exposure is described in Fig. 13.

Its resulting curve evolves in an opposite way compared to that of the characteristic $V_{rd} = f(\alpha)$ illustrated in Fig. 12, that it means it increases slightly, when $\alpha \leq 30^\circ$, increases strictly when $30^\circ < \alpha < 60^\circ$ then rises again slightly when the inclination angle is between 60 and 90° .

So that a residual water droplet can have its volume decrease with the increase in the surface's inclination angle

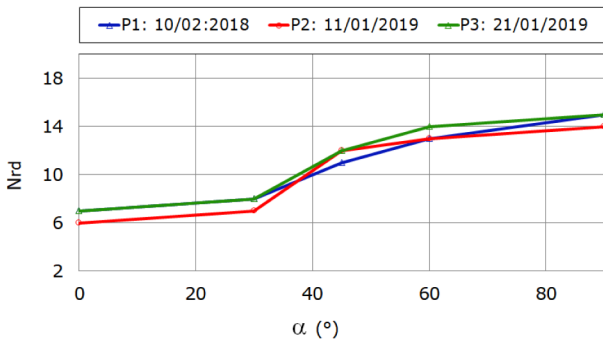
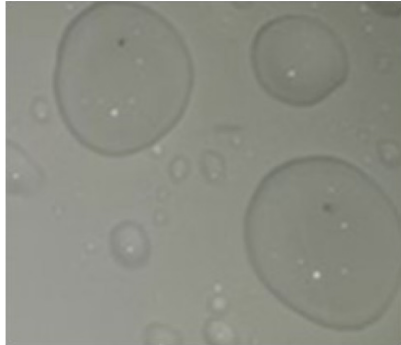


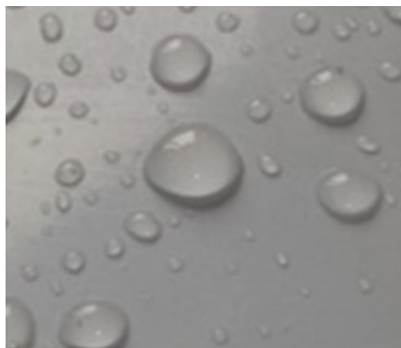
Fig. 13 Number of residual rainwater drops collected on the S_1 area of the insulation depending on the angle of its inclination and the period of its exposure

on which it rests and fulfil the new conditions of equilibrium, the only possible solution is that the rainwater drops initially impacting the surface of the insulation at this new angle of fall must be subdivided into several parts which can remain stationary on it, as shown in Fig. 14.

In summary, when the insulation's inclination angle increases, while the volume of natural rainwater drops landing on its surface decreases, their number increases regardless of the time period of its exposure to it.



(a)



(b)

Fig. 14 Size and number of residual rainwater drops collected on the surface of area S_1 of the insulation depending on the inclination angle (a) $\alpha = 0^\circ$, (b) $\alpha = 90^\circ$

3.2 Humidity rate effect of an inclined insulation on its electrical performance in the laboratory

The evolution of the humidification's intensity of the insulation's surface as a function of its inclination angle, the volume initially deposited and the level of voltage applied to the insulation, are illustrated in Figs. 15–17.

The characteristic's curve $V_{rd} = f(\alpha, V_{di})$, illustrated by Figs. 16–18, can be subdivided into three distinct zones. In the first zone, the curve is in the form of a bearing parallel to the axis of the inclination angles and extends in the

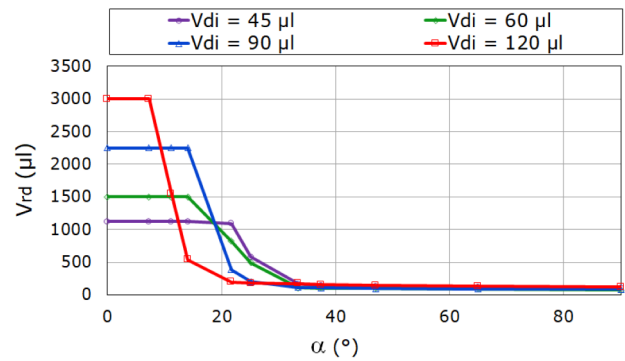


Fig. 15 $V_{rd} = f(\alpha, V_{di})$ of de-energized silicone insulation

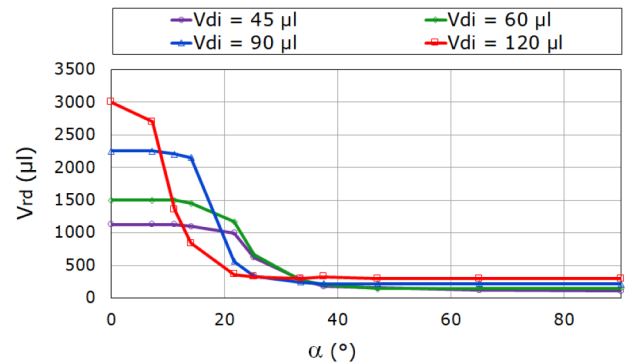


Fig. 16 $V_{rd} = f(\alpha, V_{di})$ of a silicone insulation under an alternating voltage stress equal to 10 kV

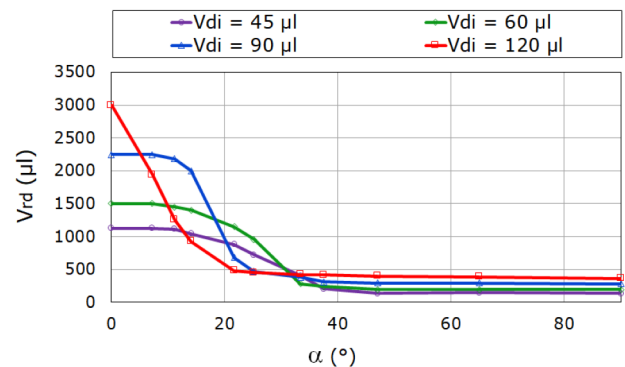


Fig. 17 $V_{rd} = f(\alpha, V_{di})$ of a silicone insulation under an alternating voltage constraint equal to 28 kV

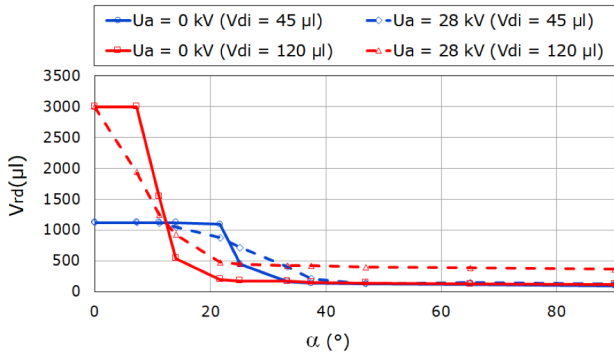


Fig. 18 Comparison of the residual water drops' volumes covering the same insulation without voltage ($U_a = 0$ kV) and under voltage ($U_a = 28$ kV)

increasing direction of the inclination angle of the insulation's surface up to $\alpha < 25^\circ$ and in the decreasing direction of the water drops' volume initially deposited (V_{di}).

This bearing corresponds to a constant volume of residual water drops and is obtained only when the insulation is de-energized (Fig. 15). This means that at an inclination angle less than 25° , the water drops keep their initial volume (V_{di}), they do not fall but only lengthen under the action of all the forces described by the Eq. (10).

On the other hand, when the insulation is placed under a voltage level, a decline of the bearing is observed, and it is increased with the increase in the water drops' volume initially deposited and the level of voltage applied to the insulation as shown in Fig. 16 and Fig. 17. The decay of the bearing under voltage level of the insulation means that at the same insulation's inclination angle, the residual volume of water drop remaining in equilibrium under voltage is less than that of the water drop retaining its balance out of voltage (Fig. 18). This volume decreases with increasing level of voltage applied to the insulation. This can be explained by the fact that under the application of an electric field to the insulation, the water drops become polarized and an electrostatic force, thus created [25, 26], is added to the balance of the generated forces according to Eq. (11).

$$mg \sin \alpha + F_e = F_{ad} + F_s + F_d \quad (11)$$

For an individual drop resting on insulation and placed under the action of an electric field, the expression of this electric force is of the form [27]:

$$F_e = \rho_t E - \frac{1}{2} |E|^2 \nabla \varepsilon + \frac{1}{2} \nabla \left(|E|^2 \frac{d\varepsilon}{d\rho_m} \rho_m \right), \quad (12)$$

where E , ρ_t , ε and ρ_m represent respectively the electric field, the total charge, the absolute permittivity of water and the volume density.

The three terms on the right side of Eq. (12) represent respectively, the Coulomb force, the dielectrophoretic force, and the electrostriction pressure. In this study, the last two terms are considered negligible due to the uniformity of the electric field between the plane and parallel electrodes. Therefore, the electrostatic force acting on an individual water droplet of the insulation is reduced to the Coulomb force.

In the case of several water drops (Fig. 4 (a)), to the Coulomb force are added the forces of mutual attraction between the drops in a row perpendicular to the electrodes and of repulsion of the water drops of a row parallel to them [28]. As the water drops in any row move almost parallel to the direction of the applied field, so the repulsive forces are considered negligible in this case [28]. Therefore, the active electrostatic forces acting on any water drop in any row are the Coulomb force and the forces of mutual attraction (F_a) between adjacent drops. For a water drop close to one of the electrodes, Eq. (12) can therefore be written in the following form:

$$F_e = \rho_t E + F_a. \quad (13)$$

In this case, Eq. (6) becomes:

$$\rho \left(\frac{\partial \vec{V}_f}{\partial t} + \vec{V}_f \cdot \nabla \vec{V}_f \right) = mg \sin \alpha + F_e - F_{ad} - F_s - F_d. \quad (14)$$

Equation (11) is written as:

$$mg \sin \alpha + \rho E = F_{ad} + F_s + F_d + F_a. \quad (15)$$

In AC voltage, the electric field changes direction at the end of each alternation, so the Coulomb force can be in the same direction as $mg \sin \alpha$ and in the opposite direction during the negative alternation. When the gravitational force and the Coulomb force are in the same direction, they can pull more water out of the initial drop than when the weight of the drop acts on its own. This explains the inferiority of the residual volume of the drop resting in equilibrium on insulation under voltage compared to that off and the greater the intensity of the Coulomb force, the smaller the residual volume becomes (Fig. 16 and Fig. 17). As a result, the surface is less humidified when the insulation is under voltage than when it is not. In this case, insulation of an already humidified power line can be more easily short-circuited when it is under voltage than insulation of the same humidified line while it is energized.

In the second zone, the shape of the characteristic is strictly decreasing, but the residual volume of water drops is greater when the insulation is energized than when it

is not (Fig. 18). Indeed, the electric field changes polarity at each alternation, so the resulting electric force is sometimes in the same direction as the force of gravitation, sometimes in the opposite direction. In this range of insulation's inclination angle, when the Coulomb force is opposed to the weight and added to the other forces, the amount of water released will be smaller and the volume retained will be larger. This phenomenon can occur with each alternation so that the residual volume is higher under voltage than without it. Contrary to the previous case, it is to be noted in this zone a higher rate of humidification for insulation under voltage than that without voltage.

In the third zone, the characteristic $V_{rd} = f(\alpha, V_{di})$ in Figs. 15–17 present a shape in the form of a bearing parallel to the axis of the inclination angles while extending in the increasing direction up to $\alpha \leq 90^\circ$ and in the descending direction of V_{di} . In addition, it should be noted that in this zone, the insulation's creepage distance is also more humidified when it is energized than when it is not. The explanation attributed to this phenomenon is also similar to that given in the case of the second zone. Finally, we can conclude that the characteristic $V_{rd} = f(\alpha, P)$ of a de-energized insulation exposed to natural rain, is qualitatively similar to the characteristic $V_{rd} = f(\alpha, V_{di})$ obtained in the laboratory in the absence or under AC voltage stress.

The characteristic giving the number of residual water drops (N_{rd}), collected on the surface of the insulation off and/or under voltage, as a function of (α) and (V_{di}) is illustrated respectively by Figs. 19–21. Its resulting shape evolves in an opposite way compared to that of the characteristic $V_{rd} = f(\alpha, V_{di})$, that it means, it is practically constant or increases very slightly when $\alpha < 25^\circ$, increases strictly when $25^\circ < \alpha < 50^\circ$ then rises again slightly when the insulation's inclination angle is between 50 and 90° .

The decrease in the volume of residual water drops with increasing angle (α) is subordinate to the subdivision of the initial drop into several parts. This subdivision is due,

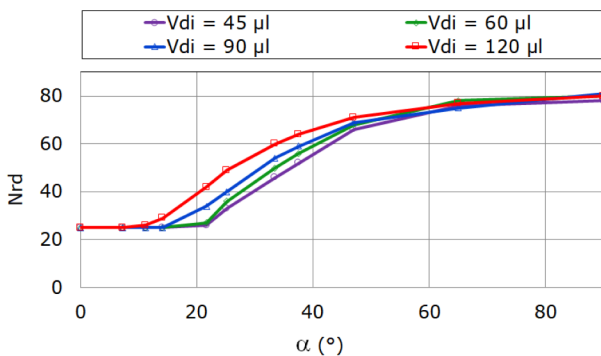


Fig. 19 $N_{rd} = f(\alpha, V_{di})$ of a de-energized silicone insulation

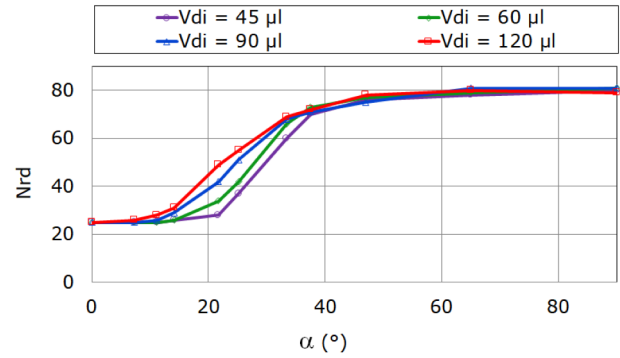


Fig. 20 $N_{rd} = f(\alpha, V_{di})$ of a silicone insulation under voltage ($U_q = 28$ kV)

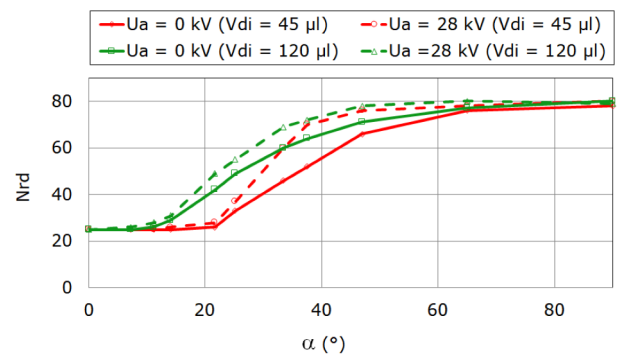


Fig. 21 Comparison of the number of residual water drops covering the same insulation without voltage ($U_a = 0$ kV) and under voltage ($U_a = 28$ kV)

on the one hand, to the forces acting on the initial drop moving on the inclined insulation, without or with voltage according to Eq. (6) or Eq. (14). On the other hand, the residual water drops created on the insulation with or without voltage must meet the equilibrium conditions described by Eq. (10) or Eq. (15).

Fig. 21 shows that the number of residual water drops is higher for insulation under voltage than that in the absence of this one. In other words, this confirms what was said previously on this subject about the volume of the residual water drops. Finally, it should be noted that the appearance of the characteristics $N_{rd} = f(\alpha, P)$ and $N_{rd} = f(\alpha, V_{di})$ is almost similar, obtained respectively on site and in the laboratory.

Fig. 22 illustrates the quantification of the simultaneous effect of the inclination angle (α) of the silicone insulation and the volume of 5 rows \times 5 water drop zigzag arrangement covering it on its electrical performance.

The resulting characteristic's curve $U_f = f(\alpha, V_{di})$ is practically V shape with a flattened right end.

When $45 \mu\text{l} \leq V_{di} \leq 90 \mu\text{l}$, the insulation flashover voltage's curve as a function of its inclination angle has a minimum for the same angle (α) regardless of the volume (V_{di}) of the water drops initially deposited. The position of this minimum is shifted to lower inclination angles with increasing

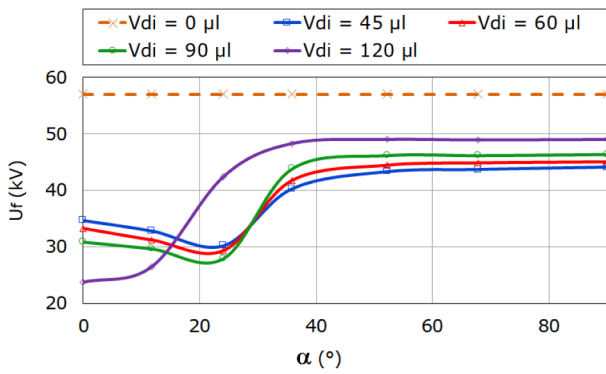


Fig. 22 $U_f = f(\alpha, V_{di})$ of silicone insulation (5 rows \times 5 zigzag water drops, $\sigma_v = 30 \mu\text{S/cm}$, $L_c = 6 \text{ cm}$, $L_{dd} = L_{de} = 1 \text{ cm}$ and $l_{rr} = 2 \text{ cm}$)

water droplet size ($0^\circ \leq \alpha < 25^\circ$). The value of the minimum flashover voltage of the insulation decreases with the approach of the value of the angle (α) to 0° and the increase of the value of (V_{di}). This angle interval is very unfavorable for the sizing of the insulator sheds, given the drastic drop in their electrical performance compared to that obtained in the dry state. Its lowest value is around 42%.

This low value of the electrical performance of the insulation is explained by a maximum elongation of the water drops along its creepage distance to a point of forming streams of water under the combined action of gravitational forces and electrohydrodynamic ones. This result in the maximum short-circuits of the insulation's creepage distance (Fig. 23). The electric flashover discharge of its surface appears at a lower value of the voltage applied to this surface. These results are similar to those obtained by other researchers [15, 16].

In the interval of insulation's inclination angle between 25 and 50° , in the wet case, the electrical performance is strictly increasing. Its maximum value can reach 86% of that obtained in the dry one. In the most favorable angle interval ($50^\circ \leq \alpha \leq 90^\circ$) is that which corresponds to an almost constant flashover voltage of the insulation and equal to 86% of that obtained in the dry case. This is due to the minimal rate of wetting of the insulation's surface by tiny residual water droplets covering it (Fig. 24). These results are in very good agreement with those obtained with standard insulators under rain [16]. Therefore, it is advisable to use this inclination angle interval for sizing the insulators' sheds, given their insulation power set at its optimum value in this case.

4 Conclusion

The results obtained from the exposure of hydrophobic silicone insulation samples during three time periods, under natural rain and unfavorable climatic conditions, lead to the following conclusions:

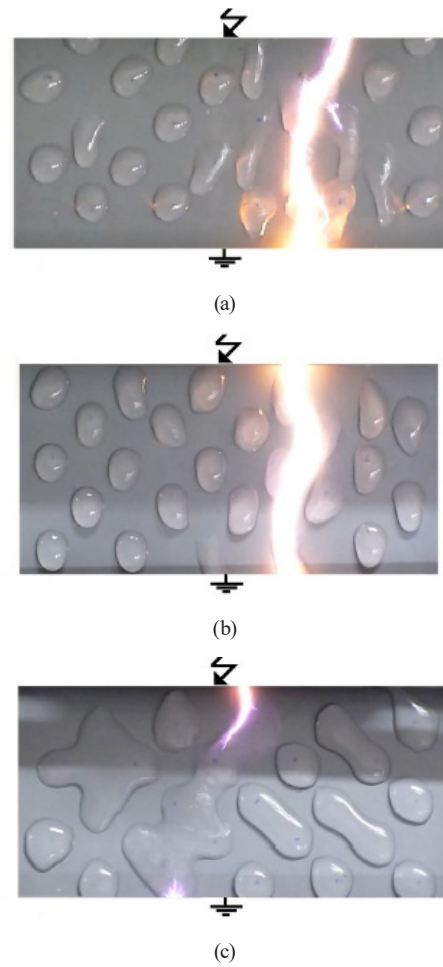


Fig. 23 Maximum elongation of water drops according to their volume when the insulation is short-circuited ($0^\circ \leq \alpha < 25^\circ$) (a) $V_{di} = 60 \mu\text{l}$, (b) $V_{di} = 90 \mu\text{l}$, (c) $V_{di} = 120 \mu\text{l}$

- Existence of creepage distance of the insulation at very high natural rain humidification rate. It can be the site of flashover by an electric discharge if it is energized.
- Decline in the humidification's degree of this creepage distance with the increase in the inclination angle compared to the horizontal of the insulation under the effect of all the essential gravitational and hydrodynamic forces of the residual rainwater drops covering its surface.
- Demonstration of two intervals of critical insulation's inclination angles, the use of the first one of which is very unfavorable for the sizing of the insulators' sheds due to the drastic reduction in the power of their insulation. However, the use of the second one is very favorable for their electrical performance because of the proximity of its value to that of the same insulators in the dry case.
- Lack of the time period of natural rain influence on the degree of humidification of the insulation creepage distance under practically similar climatic conditions.

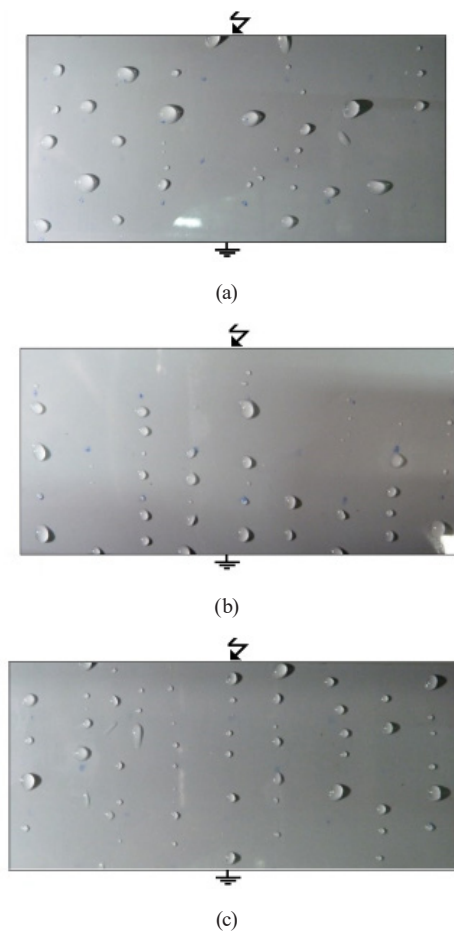


Fig. 24 Constellation of residual water drops as a function of the initial volume V_{di} in the inclination interval $50^\circ \leq \alpha < 90^\circ$, (a) $V_{di} = 60 \mu\text{l}$, (b) $V_{di} = 90 \mu\text{l}$, (c) $V_{di} = 120 \mu\text{l}$

- The results of the tests reproduced in the laboratory are summarized in the following points:
- Decline in the intensity of the insulation's surface humidification with the increase of its inclination angle, regardless of the water drops volume deposit and the level of voltage applied to this one.
- Qualitative similarity of the appearance of the two characteristics $V_{rd} = f(\alpha)$ obtained on site and in the laboratory. The only difference is in the way the surface of the insulation is wetted.
- Demonstration of a minimum by the curve of the electrical performance of a silicone insulation as a function of its inclination angle, depending on the volume deposit of water drops. The corresponding critical inclination angle belongs to an unfavorable angle interval for the sizing of insulators due to the drastic drop in their performance.
- Existence of another inclination angle interval very favorable for the insulation power of the humidified insulators due to its approximation to that obtained in the dry case.

Acknowledgements

The authors would like to express their deepest gratitude to all the members of the HV laboratory of Bejaia and the General Directorate of Scientific Research and Technological Development as a sponsoring institution. The authors are also extremely grateful to the members of the laboratory of HV in Zittau, Germany.

References

- [1] Dong, B., Jiang, X., Zhang, Z., Hu, J., Hu, Q., Shu, L. "Effect of Environment Factors on AC Flashover Performance of 3 Units of Polluted Insulator Strings under Natural Fog Condition", IEEE Transaction on Dielectrics and Electrical Insulation, 21(4), pp. 1926–1932, 2014. <https://doi.org/10.1109/TDEI.2014.004214>
- [2] Jia, Z., Chen, C., Wang, X., Lu, H., Yang, C., Li, T. "Leakage Current Analysis on RTV Coated Porcelain Insulators during Long Term Fog Experiments", IEEE Transaction on Dielectrics and Electrical Insulation, 21(4), pp. 1547–1553, 2014. <https://doi.org/10.1109/TDEI.2014.004289>
- [3] Boudissa, R., Bayadi, A., Baersch, R. "Effect of Pollution Distribution Class on Insulators Flashover under AC Voltage", Electric Power Systems Research, 104, pp. 176–182, 2013. <https://doi.org/10.1016/j.epsr.2013.06.009>
- [4] Hackam, R. "Outdoor HV Composite polymeric Insulators", IEEE Transaction on Dielectrics and Electrical Insulation, 6(5), pp. 557–585, 1999. <https://doi.org/10.1109/TDEI.1999.9286745>
- [5] Cherney, E. A., Gorur, R. S. "RTV Silicone Rubber Coatings for outdoor Insulators", IEEE Transactions on Dielectrics and Electrical Insulation, 6(5), pp. 605–611, 1999. <https://doi.org/10.1109/TDEI.1999.9286764>
- [6] Bar, C., Barsch, R., Hergert, A., Kindersberger, J. "Evaluation of the Retention and Recovery of the hydrophobicity of Insulating Materials in High Voltage Outdoor Applications under AC and DC Stresses With the Dynamic Drop Test", IEEE Transactions on Dielectrics and Electrical Insulation, 23(1), pp. 294–303, 2016. <https://doi.org/10.1109/TDEI.2015.005348>
- [7] Ghunem, R. A. "Using the Inclined-Plane Test to Evaluate the Resistance of Outdoor Polymer Insulating Materials to Electrical Tracking and Erosion", IEEE Electrical Insulation Magazine, 31(5), pp. 16–22, 2015. <https://doi.org/10.1109/MEI.2015.7214441>
- [8] Du, B. X., Liu, Y. "Pattern Analysis of Discharge Characteristics for Hydrophobicity Evaluation of Polymer Insulator", IEEE Transactions on Dielectrics and Electrical Insulation, 18(1), pp. 114–121, 2011. <https://doi.org/10.1109/TDEI.2011.5704500>

- [9] Arshad, Nekahi, A., McMeekin, S. G., Farzaneh, M. "Measurement of surface resistance of silicone rubber sheets under polluted and dry band conditions", *Electrical Engineering*, 100(3), pp. 1729–1738, 2018.
<https://doi.org/10.1007/s00202-017-0652-x>
- [10] Ren, A., Liu, H., Wei, J., Li, Q. "Natural Contamination and Surface Flashover on Silicone Rubber Surface under Haze-Fog Environment", *Energies*, 10(10), 1580, 2017.
<https://doi.org/10.3390/en10101580>
- [11] Sakoda, T., Tabira, K., Miyake, T., Hayashi, N., Haji, K., Aka, Y., Anjiki, T., Fukano, T. "Discharge behavior and dielectric performance of artificially polluted hydrophobic silicone rubber", *Journal of Electrostatics*, 93, pp. 97–103, 2018.
<https://doi.org/10.1016/j.elstat.2018.04.006>
- [12] Boudissa, R., Bouchelga, F., Kornhuber, S., Haim, K. D. "Constellation of Condensation and Raindrops and Its Effect on the DC Flashover Voltage of Inclined Silicone Insulation", *Energies*, 12(18), 3549, 2019.
<https://doi.org/10.3390/en12183549>
- [13] Jiang, Z., Jiang, X., Zhang, Z., Guo, Y., Li, Y. "Investigating the Effect of Rainfall Parameters on the Self-Cleaning of Polluted Suspension Insulators: Insight from Southern China", *Energies*, 10(5), 601, 2017.
<https://doi.org/10.3390/en10050601>
- [14] Boudissa, R., Belhoul, T., Haim, K. D., Kornhuber, S. "Effect of Inclination Angle of Hydrophobic Silicone Insulation Covered by Water Drops on its DC Performance", *IEEE Transactions on Dielectrics and Electrical Insulation*, 24(5), pp. 2890–2900, 2017.
<https://doi.org/10.1109/TDEI.2017.006543>
- [15] Bretuj, W., Fleszynski, J., Wiczorek, K. "Influence of non-ceramic insulators' shed inclination on their long-term behaviour in cyclic rain and fog conditions", In: 2007 IEEE International Conference on Solid Dielectrics, Winchester, UK, 2007, pp. 126–129. ISBN 1-4244-0750-8
<https://doi.org/10.1109/ICSD.2007.4290769>
- [16] de la O, A., Gorur, R. S. "Flashover of Contaminated Nonceramic Outdoor Insulators in a Wet Atmosphere", *IEEE Transaction on Dielectrics and Electrical Insulation*, 5(6), pp. 814–823, 1998.
<https://doi.org/10.1109/94.740762>
- [17] Belhoul, T., Boudissa, R., Haim, K. D. "Comparison of the Performance of Silicone and Glass Barriers under Direct Current and Very Severe Conditions of Pollution", *IEEE Transactions on Dielectrics and Electrical Insulation*, 24(1), pp. 471–482, 2017.
<https://doi.org/10.1109/TDEI.2016.005954>
- [18] BSI "PD IEC/TS 62073:2016 Guidance on the measurement of hydrophobicity of insulator surfaces", British Standards Institution, London, UK, 2016.
<https://doi.org/10.3403/30286694>
- [19] BSI "BS EN IEC 62631-2-1:2018 Dielectric and resistive properties of solid insulating materials - Relative permittivity and dissipation factor. Technical Frequencies (0,1 Hz to 10 MHz). AC Methods", British Standards Institution, London, UK, 2018.
- [20] BSI "BS EN 60507:2014 Artificial pollution tests on high-voltage ceramic and glass insulators to be used on a.c. systems", British Standards Institution, London, UK, 2018.
- [21] Phillipow, E. "Taschenbuch Elektrotechnik in sechs Bänden: Band 6 Systeme der Electroenergietechnik" (Paperback Electrical Engineering in Six Volumes: Volume 6 Electrical Power Engineering Systems), VEB Verlag Technik, Berlin, , Germany, 1982. (in German)
- [22] Krzma, A. S., Albano, M., Haddad, A. "Flashover influence of fog rate on the characteristics of polluted silicone-rubber insulators", In: 2017 52nd International Universities Power Engineering Conference (UPEC), Heraklion, Greece, 2017, pp. 1–5. ISBN 978-1-5386-2345-9
<https://doi.org/10.1109/upec.2017.8231958>
- [23] Yilbas, B. S., Al-Sharafi, A., Ali, H., Al-Aqeeli, N. "Dynamics of a water droplet on a hydrophobic inclined surface: influence of droplet size and surface inclination angle on droplet rolling", *RSC Advances*, 7(77), pp. 48806–48818, 2017.
<https://doi.org/10.1039/C7RA09345D>
- [24] Yang, L., Sun, Y., Liao, Y., Kuang, Z., Hao, Y., Li, L., Zhang, F. "Dynamic Deformation of Pendant Drops on the Edge of High-voltage Bushing Sheds Under Extreme Rainfall", *IEEE Access*, 8, pp. 118101–118113, 2020.
<https://doi.org/10.1109/ACCESS.2020.3004878>
- [25] Li, J., Wei, Y., Huang, Z., Wang, F., Yan, X. "Investigation of the Electric Field Driven Self-propelled Motion of Water Droplets on a Super-hydrophobic Surface", *IEEE Transactions on Dielectrics and Electrical Insulation*, 23(5), pp. 3007–3015, 2016.
<https://doi.org/10.1109/TDEI.2016.7736864>
- [26] Hamour, K., Bouchelga, F., Boudissa, R., Kornhuber, S., Haim, K. D. "Optimization of the superhydrophobic insulation longevity by expulsion of any wet deposit with a weak alternating electrical field", *Journal of Electrostatics*, 105, 103451, 2020.
<https://doi.org/10.1016/j.elstat.2020.103451>
- [27] Morgan, H., Green, N. G. "AC Electrokinetics: colloids and nanoparticles", Research Studies Press, 2003. ISBN 9780863802553
- [28] Ndoumbe, J. "Étude comportementale des gouttelettes d'eau déposées sur la surface d'un isolateur composite haute tension en présence du champ électrique" (Study of the behavior of water droplets deposited on high voltage composite insulator surface in the presence of the electric field), Doctoral Thesis, École Centrale de Lyon, 2014. (in French)